Exploring the redox properties of bench-stable uranyl(VI) diamidodipyrrin complexes

Karlotta van Rees[a], Emma K. Hield[a], Ambre Carpentier[b], Laurent Maron[b], Stephen Sproules[c], and Jason B. Love*[a]

[a]EaStCHEM School of Chemistry, The University of Edinburgh, Edinburgh, EH9 3FJ, UK. [b]LPCNO, INSA, Université de Toulouse, 135, avenue de Rangueil, 31077, Toulouse cedex 4, France. [c]WestCHEM School of Chemistry, University of Glasgow, Glasgow, G12 8QQ, UK.

Dipyrrin, Radical, Reduction, Uranium, Uranyl

ABSTRACT: The uranyl complexes UO_2(OAc)(**L**) and UO_2Cl(**L**) of the redox-active, acyclic diamido-dipyrrin anion, **L**$^-$ are reported and their redox properties explored. Due to the inert nature of the complexes towards hydrolysis and oxidation, the synthesis of both ligand and complexes was conducted on the bench. Voltammetric, EPR-spectroscopic and density functional theory (DFT) studies show that the one-electron chemical reduction by the reagent $CoCp_2$ leads to the formation of a dipyrrin radical for both complexes, [Cp_2Co][UO_2(OAc)(**L**$^\bullet$)] and [Cp_2Co][UO_2Cl(**L**$^\bullet$)].

Introduction

Redox-active ligands, also referred to as redox non-innocent ligands continue to fascinate and perplex chemists. While the ability of these ligands to adopt multiple stable oxidation states often hinders the analysis of the electronic structures of metal complexes, the reactivity of metals can be expanded by their action as electron reservoirs, altered Lewis acids, reactive ligand radicals, and in enabling ligand-to-substrate electron transfer.[1-3] Although the chemistry with transition metals has been vastly explored, there has only recently been a rise in interest of actinide complexes of redox-active ligands, in particular those of uranium.[4-6]

Uranium is most commonly present as the uranyl(VI) dication, UO_2^{2+} under ambient conditions. This dioxide adopts a linear $[O{\equiv}U^{VI}{\equiv}O]^{2+}$ structure in which the axial oxygen atoms (O_{ax}) are strongly bound to the uranium center.[7] As a result, UO_2^{2+} is very stable in terms of both kinetics and thermodynamics. Even so, the reduction of uranyl(VI) to uranium(IV) via the unstable uranyl(V) cation UO_2^+ is an important aspect of uranium remediation by immobilization, and significant advances have been made in the isolation and study of reduced uranyl complexes, e.g., in oxo-metalated and oxo-silylated uranyl(V) compounds.[8]

Uranyl complexes of redox-active ligands such as Schiff-bases,[9-10] quinones,[4] and pyrroles in, for example tetraaza[14]-annulenes,[11] calix[4]pyrroles,[12] and dipyrrins,[13-15] have been reported. Due to the added redox character of these ligands the complexes react differently under reducing conditions. For example, uranyl(VI) complexes of pentadentate N_3O_2-saldien ligands with various substituents all underwent one-electron uranium reduction to afford the corresponding uranyl(V) complex, regardless of the difference in the substituents.[16] In contrast, the uranyl(VI) α-di-imine diphenolate (**1**) (Figure 1) and uranyl(VI) salophens undergo single-electron reduction of the ligand, leading to ligand-centered radical anions and not the expected uranyl(V) complexes.[9-10, 17]

Dipyrrins are popular due to their effective absorption of visible light through π-π*transitions forming colorful and luminescent metal complexes.[18-19] Uranyl complexes of dipyrrin ligands can be readily accessed through an anhydrous, salt metathesis route.[13] We recently reported the redox behavior of the donor-expanded Schiff-base dipyrrin uranyl(VI) complex (**2**) (Figure 1) and its contrasting but controlled inner-and outer-sphere redox chemistry. The use of one equivalent of the outer-sphere reductant $CoCp_2$ resulted in the one-electron reduction of the ligand to a dipyrrin radical. The addition of a second equivalent of $CoCp_2$ reduced the uranium center to uranyl(V). Reaction of **2** with one equivalent of the inner-sphere reductant $[TiCp_2Cl]_2$ led to the formation of a doubly-titanated uranium(IV) complex.[14] In addition, the effect of both the equatorial coordination sphere and the axial oxo-ligand bonding in **2** were investigated, showing that it is possible to shift the non-aqueous U(VI/V) and U(V/IV) reduction potentials to values in the range accessible to reductants that are present in uranium remediation processes and in nuclear fuel storage.[15] However, these dipyrrin complexes all display air sensitivity and therefore need to be handled accordingly.

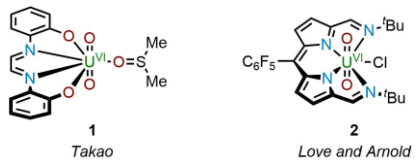

Figure 1. Structures of dipyrrin uranyl(VI) complexes.

This study presents the formation of easy-to-synthesize and bench-stable uranyl complexes of a diamidodipyrrin ligand and an evaluation of their reduction properties. A similar ligand has previously been exploited in the formation of boron and transition metal complexes, such as

nickel, copper, and cobalt, although these studies mainly focused on the rich coordination chemistry of these ligands.[20-22] We rationalized that the use these ligands would deliver a uranyl complex that would potentially be resistant towards oxidation reactions and hydrolysis, whilst maintaining its redox properties.

Results and discussion

Synthesis and structures of uranyl(VI) complexes

The synthesis of H**L** was achieved using a modification of previously reported procedures (Scheme 1).[20] The amination of the trichloroacetyl pyrrole was conducted in neat, boiling *tert*-butylamine and under reflux conditions, however, due to the steric demand of *tert*-butylamine the pyrrole amide (**4**) was synthesized in lower yield compared with the literature derivatives. The second step was an acid-catalyzed condensation which led to the formation of the dipyrromethane (**5**) in 36 % yield. In contrast to acyclic Schiff-base dipyrrin ligands made previously in our group, **5** did not spontaneously oxidize during its synthesis and required additional oxidant (DDQ) to form dipyrrin H**L** which was readily purified using silica chromatography.[23] Formation of H**L** was not only indicated by the disappearance of the *meso*-proton singlet at 5.86 ppm in the ^{1}H NMR spectrum, but also by the intensely orange solid obtained, typical of the dipyrrin chromophore (ESI).

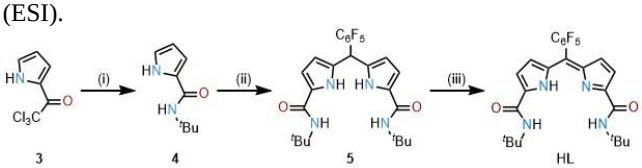

Scheme 1. Synthesis of H**L**. (i) neat ^{t}BuNH$_2$, reflux, 16 h. (ii) 0.5 equiv. pentafluorobenzaldehyde, 5 mol % *p*-TSA, PhCH$_3$, reflux, 16 h. (iii) 1.1 equiv. DDQ, THF, RT, 24 h.

Reaction between H**L**, triethylamine, and one equivalent of uranyl acetate ($UO_2(OAc)_2$•$2H_2O$) or uranyl chloride $UO_2Cl_2(THF)_2$ in a mixture of MeOH and $CHCl_3$ (1:3, v/v) led to rapid color changes from orange to a dark pink solution (Scheme 2). The acetate complex UO_2(OAc)(**L**) was obtained in 77 % yield as a dark pink solid and the chloride UO_2Cl(**L**) was obtained in 91 % yield as a dark reddish-pink solid after aqueous workups. While no additional purification steps were required for UO_2(OAc)(**L**), UO_2Cl(**L**) was heated in chloroform after the solid was obtained to ensure the formation of a single product. The second product was hypothesized to be the ion pair [UO_2(solvent)(**L**)][Cl] formed through ready dissociation of the chloride anion.[15]

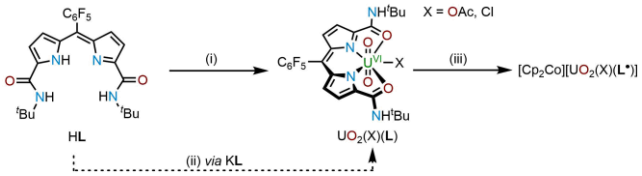

Scheme 2. Synthesis of uranyl complexes of H**L**. (i) 1.1 equiv. $UO_2(OAc)_2$•$2H_2O$ or $UO_2Cl_2(THF)_2$, NEt_3, MeOH/$CHCl_3$ (1:3, v/v), reflux, 16 h. (ii) 1.5 equiv. KH, THF, RT, 16 h. followed by the addition of $UO_2Cl_2(THF)_2$. (iii) 1 equiv. $CoCp_2$, THF, RT. 16 h.

Formation of the uranyl complexes was indicated by the disappearance of the pyrrole N-H proton at 12.69 ppm for H**L** and the downfield shift of the pyrrole peaks in the ^{1}H NMR spectra (ESI).[24] Both complexes adopt C_{2h}-symmetry in solution that is also seen in the ^{19}F NMR spectra with 3 resonances indicating horizontal planar symmetry. In addition, the ^{1}H NMR spectrum of UO_2(OAc)(**L**) contains a broad singlet at 2.17 ppm with an integration of 3H that is assigned to the coordinated acetate ion; this fluxionality of the acetate means that it is not easily identified in the ^{13}C{^{1}H} NMR spectrum. The chloride complex UO_2Cl(**L**) was also prepared under non-aqueous conditions: the reaction between K**L** (formed *in-situ* by reaction of H**L** and KH in THF) and $UO_2Cl_2(THF)_2$ in THF formed UO_2Cl(**L**) in high yield.

Crystals suitable for X-ray analysis were grown for H**L**, UO_2(OAc)(**L**), and UO_2Cl(**L**) (Figures 2 and 3). Weakly diffracting orange plates of H**L** were crystallized from a concentrated DMSO solution and the data only reveal connectivity. H**L** does not display any intermolecular hydrogen bonding and instead displays hydrogen bonding between the amide N(4)-H and the O3 atom of the DMSO solvate molecule.

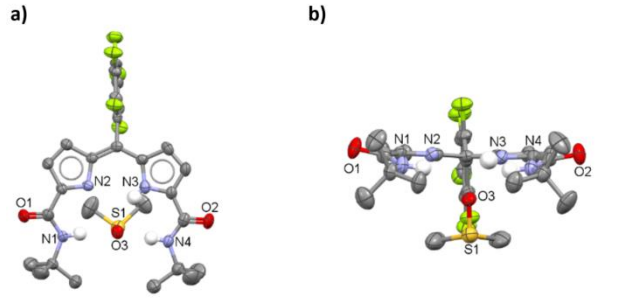

Figure 2. X-ray crystal structure of H**L** viewed from side and top. For clarity, all hydrogen atoms except those involved in hydrogen bonding are omitted (displacement ellipsoids are drawn at 50 % probability).

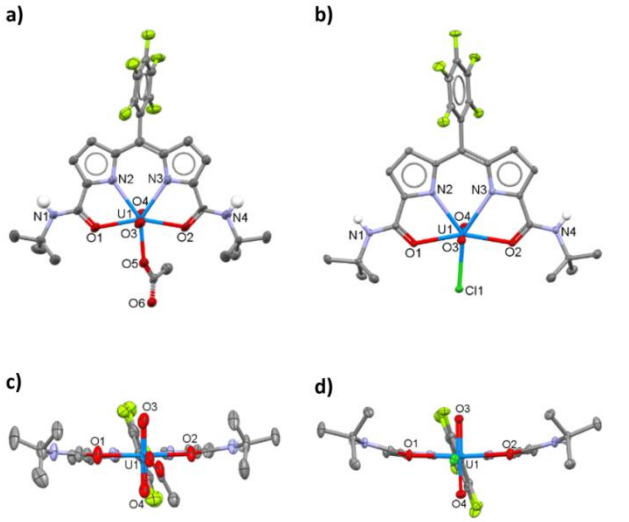

Figure 3. X-ray crystal structures of UO_2(OAc)(**L**) (a and c) and UO_2Cl(**L**) (b and d) viewed from side and top. For clarity, all hydrogen atoms except on amide N1 and N4 are omitted (displacement ellipsoids drawn at 50 % probability).

Greenish pink blocks of UO_2(OAc)(**L**) were grown through slow evaporation of a concentrated THF solution. The asymmetric unit comprises two molecules that differ primarily

in the orientation of the monodentate acetate group, supporting the fluxionality of this anion seen in solution by NMR spectroscopy. In the solid state, the complex adopts a distorted pentagonal bipyrimidal coordination geometry, in which the ONNO-donor set of the expanded dipyrrin ligand occupies the equatorial positions along with the acetate ligand. This shows similar ONNO-coordination geometry to Cu(DADP^{ph,ipr})Cl (DADP^{ph,ipr} = 1,1'-isopropylamide-5-phenyl-4,6-dipyrrinato) in which the equatorial position is occupied by a chloride ligand.[20] The uranium coordinates to the oxygen atoms of the amide groups, as seen with other uranyl(VI) amide complexes.[25] The O_{ax}(4)-U(1) and U(1)-O_{ax}(3) bonds are 1.7151(6) and 1.762(6) Å, respectively, with an O_{ax}(4)-U(1)-O_{ax}(3) angle of 177.92°, and are fully consistent with uranyl(VI). The U(1)-$N_{pyrrole}$ bond lengths are 2.614(6) and 2.504(6) Å, while the U(1)-O_{amide} bond length is 2.315(1) Å.

Pink crystals of UO_2Cl(**L**) were grown by slow evaporation of a THF solution and the X-ray crystal structure is similar to that of UO_2(OAc)(**L**). In this case, the O_{ax}(4)-U(1) and U(1)-O_{ax}(3) bonds are 1.774(2) and 1.759(2) Å, respectively, with an O_{ax}(4)-U(1)-O_{ax}(3) angle of 177.54°. The U(1)-$N_{pyrrole}$ bond lengths are 2.508(2) and 2.516(2) Å, while the U(1)-O_{amide} bond lengths are 2.389(2) and 2.406(2) Å. The U(1)-Cl(1) bond length is 2.7019(7) Å, which is close to the U-Cl bond length of the dipyrrin-diimine analogue **2**, 2.710(1) Å.[14] Both complexes exhibit U-O_{ax} bond lengths and O_{ax}-U-O_{ax} angles in the range of other unfunctionalized uranyl(VI) complexes in which an average U-O_{ax} bond is 1.777 Å is seen.[8] In addition, the U-O_{amide} bond distance is similar than those found in other uranyl(VI) amide complexes (typically 2.34–2.40 Å).[25]

Electrochemistry

The cyclic voltammograms (CVs) of H**L**, UO_2(OAc)(**L**) and UO_2Cl(**L**) were recorded in MeCN at a scan-rate of 100 mV s^{-1} (Figure 4). The CV of H**L** features a quasi-reversible reduction at $E_{1/2}$ –1.15 V *vs* Fc/Fc$^+$ and an irreversible reduction at E_p –1.99 V *vs* Fc/Fc$^+$. The first reduction appears reversible when isolated in the CV (Figure 4, dotted line). This feature is significantly less negative than that of the analogous di-imine dipyrrin ligand (seen in **2**) which displays a reversible reduction at $E_{1/2}$ –1.51 V *vs* Fc/Fc$^+$ in CH_2Cl_2.[14] Although the diamide ligand is more easily reduced than the di-imine analogue, this is not true of their corresponding complexes. The CV of UO_2(OAc)(**L**) features four different redox processes upon cathodic scanning. The first is a quasi–reversible reduction process at $E_{1/2}$ –1.10 V *vs* Fc/Fc$^+$, followed by irreversible reduction processes at E_p –1.97, –2.31, and –2.53 V *vs* Fc/Fc$^+$. The CV of UO_2Cl(**L**) also features four different redox processes, the first quasi-reversible reduction process at $E_{1/2}$ –0.88 V *vs* Fc/Fc$^+$, followed by irreversible reduction processes at E_p –1.72, –2.15, and –2.50 V *vs* Fc/Fc$^+$. In contrast, the di-imine dipyrrin analogue **2** has two consecutive quasi-reversible reduction processes that are both more accessible at $E_{1/2}$ –0.97 and –1.18V *vs* Fc/Fc$^+$ compared with UO_2(X)(**L**) (X = OAc, Cl). This variation may be due to an increase of electron density from the amide oxygen atoms to the uranium in the uranyl complexes of **L**, making them less susceptible to reduction. In addition, the solution of UO_2Cl(**L**) required additional stirring after each measurement due to the formation of a second species with similar reduction pattern (ESI) which may arise from chloride dissociation to form the ion pair [UO_2(MeCN)(**L**)][Cl].

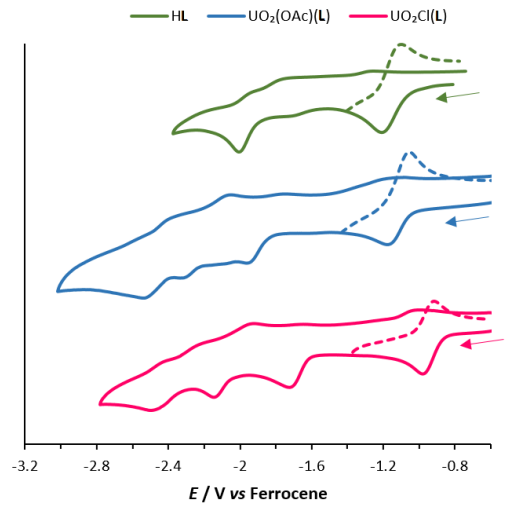

Figure 4. Stacked cyclic voltammograms for H**L**, UO_2(OAc)(**L**) and UO_2Cl(**L**). All measured as 1 mM MeCN solutions (0.1 M [^{n}Bu$_4$N][PF$_6$] supporting electrolyte, glassy-carbon working electrode, Pt gauze counter electrode and silver wire quasi-reference electrode). Potentials are referenced against the Fc/Fc$^+$ couple recorded under identical conditions.

Single-electron reduction

Colbaltocene ($CoCp_2$) is a strong outer-sphere reductant with a formal Co(III)/Co(II) redox potential of −1.33 V *vs* Fc/Fc$^+$,[26] but could only be used to study the first reduction of UO_2(OAc)(**L**) and UO_2Cl(**L**) due to the significantly more negative second reduction potentials. Reactions between either UO_2(OAc)(**L**) or UO_2Cl(**L**) and one equivalent of $CoCp_2$ in pyridine-d_5 lead to a dark red, NMR-silent compound (Scheme 2). Scale-ups were carried out in dry THF, causing the products to precipitate as greenish-brown solids which are characterized as the ligand-reduction products [Cp_2Co][UO_2(OAc)(**L**$^\bullet$)] or [Cp_2Co][UO_2Cl(**L**$^\bullet$)], respectively. Both compounds were successfully analyzed by elemental analyses but to obtain single crystals for X-ray structural characterization were unsuccessful.

EPR spectroscopy

The EPR spectra of [Cp_2Co][UO_2(OAc)(**L**$^\bullet$)] and [Cp_2Co][UO_2Cl(**L**$^\bullet$)] show a relatively sharp line devoid of hyperfine structure synonymous with the formation of an S = ½ species (ESI). Both compounds show a g_{iso} of 1.997, a value significantly shifted from that of the free electron (2.0023). These data are consistent with a ligand-centered reduction affording [UO_2(X)(**L**$^\bullet$)]$^-$, where the presence of the coordinated U(VI) ion has not only instigated the g-shift but broadens the line, obscuring all hyperfine splitting from the various spin-active nuclei in the dipyrrin.[14]

Electronic spectroscopy

The absorbance spectra of H**L**, acetate and chloride uranyl complexes UO_2(X)(**L**), and reduced complexes [Cp_2Co][UO_2(X)(**L**$^\bullet$)] were recorded (Figure 5). H**L** has a maximum absorbance of 470 nm (ε = 27 280 M^{-1} cm^{-1}) and is similar to the previously synthesized derivatives.[20] Upon

metalation to form the uranyl complexes $UO_2(X)(\mathbf{L})y$, the easy to visualize color change is reflected in the UV-vis spectrum with significant red-shifts observed relative to H**L**; the absorbance is independent of the anion and both complexes exhibit a maximum absorbance at 546 nm (ε = 82 316 M^{-1} cm^{-1}) along with a second band, weaker at 510 nm, and a shoulder at 478 nm. The reduced compounds $[Cp_2Co][UO_2(X)(\mathbf{L}^{\bullet})]$ are poorly soluble in THF and the measurements were therefore carried out in pyridine. Both compounds exhibit a near identical spectrum. The intense absorption of the dipyrrin chromophore in the UV and visible regions that took place before 300 nm, has now shifted dramatically and can be seen just before 400 nm. The maximum absorbance has also shifted to 500 nm (ε = 45 700 M^{-1} cm^{-1}).

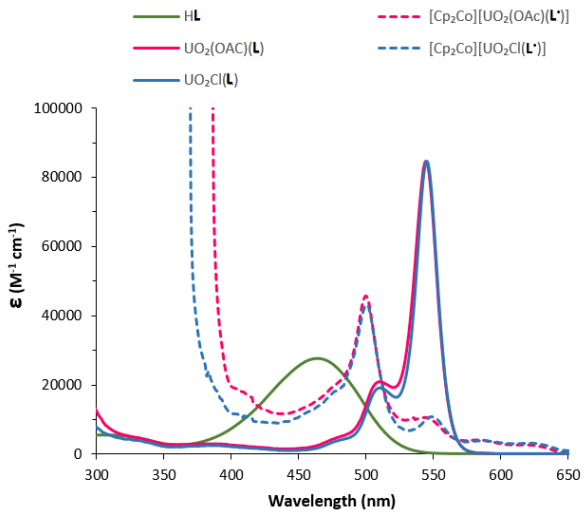

Figure 5. UV-vis spectrum of H**L** in CH_2Cl_2, $UO_2(OAc)(\mathbf{L})$ and $UO_2Cl(\mathbf{L})$ in THF, and $[Cp_2Co][UO_2(OAc)(\mathbf{L}^{\bullet})]$ and $[Cp_2Co][UO_2Cl(\mathbf{L}^{\bullet})]$ in pyridine.

DFT calculations

The occurrence of single-electron reduction of the diamidodipyrrin ligand and not the uranium center in the uranyl complexes is supported by computational analysis. DFT calculations were undertaken on both $UO_2(OAc)(\mathbf{L})$ and $UO_2Cl(\mathbf{L})$ and their one-electron reduction products. The former experiments reveal that the LUMOs of both complexes are located entirely on the ligand, whereas in contrast the LUMOs+1 are metal-based, indicating that one-electron reductions should indeed lead to ligand-based radicals (Figure 6). Furthermore, the LUMOs+1 suggest that the second reduction should lead to uranium reduction, i.e., to the formation of uranyl(V) complexes. The SOMOs of $[UO_2(OAc)(\mathbf{L}^{\bullet})]^-$ and $[UO_2Cl(\mathbf{L}^{\bullet})]^-$ are also ligand based and the unpaired spin density maps of both show that the electron density is located entirely on the *meso*-carbon of the ligand, furthermore confirming the radical character of the ligand after one-electron reduction.

As shown previously, the CV of $UO_2Cl(\mathbf{L})$ exhibits another similar set of reductions and it was concluded that this was due to the lability of the chloride, forming the ion pair $[UO_2(MeCN)(\mathbf{L})][Cl]$ in solution. A study conducted previously in the group, however, demonstrated that the cation of **2**, $[UO_2(\mathbf{L}^2)][BAr^F]$, first undergoes U(VI)/U(V) reduction, rather than the formation of a ligand radical.[15] Therefore, to ensure both $UO_2Cl(\mathbf{L})$ and $[UO_2(MeCN)(\mathbf{L})][Cl]$ exhibit similar reactivity, the LUMOs of both $UO_2Cl(\mathbf{L})$ and $[UO_2(\mathbf{L})]^+$ were compared to **2** and $[UO_2(\mathbf{L}^2)]^+$ (ESI). These calculations show that the LUMOs of both $UO_2Cl(\mathbf{L})$ and $UO_2Cl(\mathbf{L}^2)$ are ligand based. While the LUMO of $[UO_2(\mathbf{L}^2)]^+$ exhibits both ligand and metal character, and results experimentally in U(VI)/U(V) reduction, the LUMO of $[UO_2(\mathbf{L})]^+$ is fully ligand based. This supports that the second species seen in the CV is likely the ion pair $[UO_2(MeCN)(\mathbf{L})][Cl]$ and that this compound exhibits the same reactivity as the parent $UO_2Cl(\mathbf{L})$.

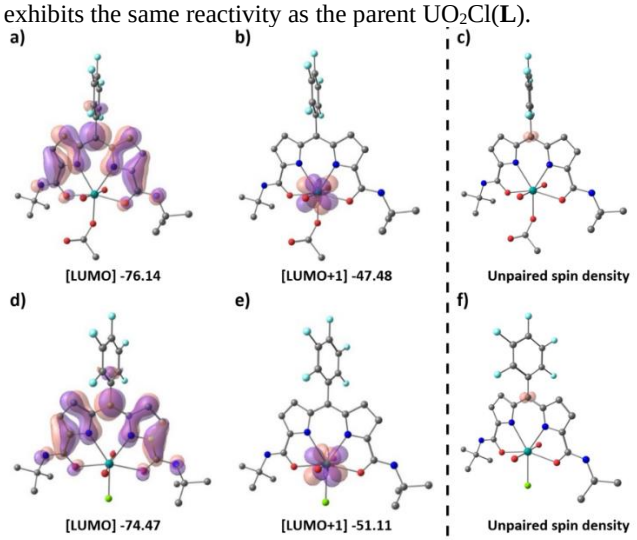

Figure 6. Molecular orbital plots of $UO_2(OAc)(\mathbf{L})$ (a and b) and $UO_2Cl(\mathbf{L})$ (d and e). ISO value of 0.02 au. Hydrogen atoms were omitted for clarity. Positive is purple; negative is red. All energies are depicted in kcal mol^{-1}. c and f showing the unpaired spin densities of $[UO_2(X)(\mathbf{L}^{\bullet})]^-$.

Conclusions

The diamido dipyrrinm ligand acts as a tetradentate chelate for the uranyl dication and, due to its low lying π*-MOs, is a non-innocent redox partner in the reduction chemistry of its uranyl complexes. The uranyl complexes $UO_2(OAc)(\mathbf{L})$ and $UO_2Cl(\mathbf{L})$ are both insensitive towards hydrolysis and could therefore be easily prepared and stored on the bench. In addition, both complexes undergo one-electron reduction when reacted with $CoCp_2$, leading to ligand radicals rather than uranyl(V) complexes. Although attempts to crystallize the singly reduced complexes were unsuccessful, EPR, CV and DFT studies support the presence of a ligand radical. Our current investigations are focused on manipulating the redox-behavior of similar dipyrrin ligands in order to form air-stable uranyl(V) dipyrrin complexes.

Experimental section

General procedure

Caution: Depleted uranium (primary isotope ^{238}U) is a weak α-emitter (4.197 MeV) with a half-life of 4.47×109 years. Manipulations and reactions should be carried out in monitored fume hoods or in an inert atmosphere glovebox in a radiation laboratory equipped with α- and β-counting equipment. The syntheses of all air- and moisture-sensitive compounds were carried out using standard Schlenk techniques

under an atmosphere of dry argon. Vacuum Atmospheres and MBraun glove boxes were used to manipulate and store air- and moisture-sensitive compounds under an atmosphere of dried and deoxygenated dinitrogen. The solvents pyridine-d_5 and THF-d_8 were refluxed over potassium metal overnight, trap-to-trap distilled and three times free-pump-thaw degassed prior to use. All glassware was dried in an oven at 160 °C, cooled under 10-3 mbar vacuum and then purged with argon. Prior to use, all Fisherbrand R 1.2 mm retention glass microfiber filters and stainless-steel cannula were dried in an oven at 160 °C overnight. All solvents for use with air- and moisture-sensitive compounds were stored in Teflon-tapped ampoules containing pre-dried 4 Å molecular sieves. Solvents were collected from a solvent purification system (Innovation Technologies), where they had been passed over a column of molecular sieves for 24 hours prior to collection. They were then degassed prior to use and subsequent storage. All chemicals were used as used as received without any purification, unless otherwise specified. Tetrabutylammonium hexafluorophosphate, [^{n}Bu$_4$N][PF$_6$], was recrystallized twice from absolute ethanol and further dried for two days under vacuum.

^{1}H NMR spectra were recorded on a Bruker AVA400 spectrometer operating at 399.90 MHz, a Bruker AVA500 or Bruker PRO500 operating at 500.12 MHz or a Bruker AVA600 spectrometer operating at 599.81 MHz. ^{13}C{^{1}H} NMR spectra were recorded on a Bruker AVA500 or Bruker PRO500 operating at 125.76 MHz. ^{19}F{^{1}H} NMR spectra were recorded on a Bruker AVA500 spectrometer operating at 470.59 MHz. Chemical shifts are reported in parts per million (ppm). ^{1}H and ^{13}C{^{1}H} NMR spectra are referenced to residual solvent resonances calibrated against an external standard, SiMe$_4$ (d = 0 ppm). ^{19}F{^{1}H} NMR spectra are referenced to an external standard, CCl$_3$F (d = 0 ppm). All spectra were recorded at 298 K unless otherwise specified. All data were processed using MestReNova 12.0.3. Full assignment in the supplementary information.

Single crystal X-ray diffraction data were collected at 120 K on an Oxford Diffraction Excalibur diffractometer using graphite monochromated Mo-Ka radiation equipped with an Eos CCD detector (λ = 0.71073 Å), or at 120 K on a Supernova, Dual, Cu at Zero Atlas diffractometer using Cu-Kalpha radiation (λ = 1.5418 Å). Structures were solved using ShelXT direct methods or intrinsic phasing and refined using a full-matrix least square refinement on $|F|^2$ using ShelXL.[27-29] All programs were used within the Olex suite.[30] All non-hydrogen atoms refined with anisotropic displacement parameters and H-parameters were constrained to parent atoms and refined using a riding model unless otherwise specified. All X-ray crystal structures were analyzed and illustrated using Mercury 4.3.1.

Elemental analyses were carried out by Elemental Microanalysis Ltd., measured in duplicate. All FT-IR spectra were recorded using JASCO 410 or JASCO 460 plus spectrometers. Intensities are assigned as: w = weak, m = medium, and s = strong. All UV-vis absorption spectra were recorded on a Jasco V-670 spectrometer on a 10 mm quartz cuvette, fitted with a septum for air-sensitive compounds.

Synthesis

4: Trichloroacetylpyrrole (4.8 g, 23 mmol, 1.0 eq.) was added to 50 mL of freshly distilled tert-butylamine, and the mixture was heated to 50 °C for 48 h. Solvent was removed under reduced pressure. Solid was washed with *n*-hexane (3 x 100 mL) and the remaining white solid was recrystallized from a hot EtOH solution. Yield = 1.42 g (39 %) ^{1}H NMR (400 MHz, Methanol-d_4): δ_H 6.86 (1H, dd, *J* = 2.6 1.4 Hz), 6.75 (1H, dd, *J* = 3.7, 1.4 Hz), 6.12 (1H, dd, *J* = 3.7, 2.6 Hz), 1.43 (9H, s). ^{13}C{^{1}H} NMR (101 MHz, Methanol-d_4): δ_C 158.51, 126.50, 120.95, 110.34, 108.56, 50.80, 27.90. HRMS (ESI$^+$, MeOH): *m*/*z* C$_9$H$_{15}$N$_2$O [M+H]$^+$ requires 167.117890, found 167.11770 (mass error = –0.19 ppm). EA: C$_9$H$_{14}$N$_2$O (MW = 166.2 gmol^{-1}) requires C,65.03 %; H,8.49 %; N,16.85 %. Found: C,64.91 %; H,8.62 %; N,16.92 %. FTIR (film) ν_{MAX} 1581 cm^{-1} C(5)=ONH.

5: **4** (2.2 g, 14.7 mmol, 2.0 eq.) was added to PhCH$_3$ (80 mL). Pentafluorphenylbenzaldehyde (1.5 g, 7.6 mmol, 1.0 eq.) and *p*-TSA (40 mg, 0.23 mmol, 0.03 eq.) were added to the grey suspension before the mixture was set to reflux. After 20 h the reaction was cooled back to RT. The solids were filtered and washed with PhCH$_3$ (3 x 10 mL). The isolated white solid was recrystallized from *n*-hexane, resulting in a white powder. Yield = 1.45 g (36 %) ^{1}H NMR (400 MHz, Dimethylsulfoxide-d_6): δ_H 11.33 (2H, s), 7.21 (2H, s, 2H), 6.70 (2H, dd, *J* = 3.7, 2.5 Hz), 5.86 (1H, s), 5.73 (2H, t, *J* = 3.1 Hz), 1.34 (s, 18H). ^{13}C{^{1}H} NMR (101 MHz, Dimethylsulfoxide-d_6): δ_C 160.81, 146.50, 141.97, 132.71, 127.36, 116.13, 110.54, 108.49, 108.03, 50.87, 32.96, 29.33. ^{19}F{^{1}H} NMR (376 MHz, Dimethylsulfoxide-d_6): δ_F –141.28 (2F, dd, *J* = 24.0, 6.9 Hz), –157.60 (1F, t, *J* = 22.7 Hz), –163.31 (2F, td, *J* = 23.7, 7.0 Hz). HRMS (ESI$^+$, MeOH): *m*/*z* C$_{25}$H$_{28}$F$_5$N$_4$O$_2$ [M+H]$^+$ requires 511.21269, found 511.21180 (mass error = –0.89 ppm), C$_{25}$H$_{27}$F$_5$N$_4$O$_2$Na [M+Na]$^+$ requires 533.19436, found 533.19280 (mass error = –1.84 ppm). EA: C$_{25}$H$_{27}$F$_5$N$_4$O$_2$ (MW = 510.2 gmol^{-1}) requires C,58.82 %; H,5.33 %; N,10.97 %. Found C,58.95 %; H,5.36 %; N,10.85 %. FTIR (film) ν_{MAX} 1580 cm^{-1} C(5)=ONH.

H**L**: **2** (950 mg, 1.86 mmol, 1.0 eq.) was dissolved in THF (150 mL). DDQ (460 mg, 2.02 mmol, 1.1 eq.) dissolved in THF (100 mL) was slowly added over a period of 20 minutes. The then dark-greenish yellow solution slowly turned dark red. After 22 h, the mixture was concentrated, redissolved in CH$_2$Cl$_2$ (50 mL) and filtered. The filtrate was concentrated. The crude product was purified by silica column chromatography (1 = 100 % CH$_2$Cl$_2$; 2 = 98:2 CH$_2$Cl$_2$:EtOH; rf =0.3; bright pinking orange fraction) resulting in a bright greenish orange solid. Orange single crystals suitable for X-ray crystallography were obtained through slow evaporation of a concentration DMSO solution. Yield = 240 mg (25 %). ^{1}H NMR (400 MHz, Chloroform-*d*) δ_H 12.69 (1H, bs), 6.77 (2H, d, *J* = 4.4 Hz), 6.60 (2H, bs), 6.51 (2H, d, *J* = 4.4 Hz), 1.53 (18H, s). ^{13}C{^{1}H} NMR (101 MHz, Chloroform-*d*) δ_C 159.89, 151.45, 145.88, 143.42, 141.28, 138.70, 137.77, 127.97, 125.63, 117.88, 51.79, 28.75. ^{19}F{^{1}H} NMR (376 MHz, Chloroform-*d*): δ_F –132.11 - –142.09 (2F, m), –151.07 (1F, t, *J* = 21.1 Hz), –157.37 - –166.39 (2F, m). HRMS (ESI$^+$, MeOH): *m*/*z* C$_{25}$H$_{26}$F$_5$N$_4$O$_2$ [M+H]$^+$ requires 509.19704, found 509.19419 (mass error = –2.94 ppm), C$_{25}$H$_{25}$F$_5$N$_4$O$_2$Na [M+Na]$^+$ requires 531.17899, found 531.17700 (mass error = –1.99 ppm). EA for C$_{25}$H$_{25}$F$_5$N$_4$O$_2$ (MW = 508.2 gmol^{-1}) requires C,59.05 %; H,4.96 %; N,11.02 %. Found C,58.93 %; H,4.94 %; N,10.94 %. FTIR (film) ν_{MAX} 1652 cm^{-1} C(5)=ONH. UV-vis (CH$_2$Cl$_2$): λ 252 nm, ε = 19,500 M^{-1} cm^{-1}; λ_{max} 470 nm, ε = 27 280 M^{-1} cm^{-1}.

UO$_2$(OAc)(**L**): A solution of H**L** (100 mg, 0.197 mmol, 1 eq.; in MeOH:CHCl$_3$, 1:3, 70 mL) was added to a

solution of $UO_2(OAc)_2$•$2H_2O$ (91.8 mg, 0.217 mmol, 1.1 eq.; in MeOH:$CHCl_3$, 1:3, 20 mL) after which NEt_3 was added (36 µL, 0.256 mmol, 1.3 eq.), causing an immediate colour change from orange to pink. The reaction mixture was heated to 65 °C and stirred for 18 h, after which solvent was removed under reduced pressure. The oil was redissolved in CH_2Cl_2 (75 mL), washed with H_2O (3 x 15 mL) and dried with $MgSO_4$. A greenish pink solid was obtained. Greenish-pink single crystals suitable for X-ray crystallography were obtained through slow evaporation of a concentrated THF solution. Yield = 127 mg (77 %). ^{1}H NMR (400 MHz, Methanol-d_4): δ_H 7.59 (2H, d, J = 4.5 Hz), 7.15 (2H, d, J = 4.5 Hz), 2.17 (3H, bs), 1.80 (18H, s). ^{13}C{^{1}H} NMR (126 MHz, Methanol-d_4): δ_C 169.76, 158.86, 144.80, 143.44, 142.21, 137.67, 137.41, 133.53, 128.46, 119.00, 54.04, 27.70. ^{19}F{^{1}H} NMR (376 MHz, Methanol-d_4): δ_F –141.82 (2F, dd, J = 21.3, 5.9 Hz), –155.06 (1F, t, J = 20.6 Hz), –163.97 (2F, td, J = 20.7, 6.0 Hz). HRMS (ESI$^+$, MeOH): m/z $C_{27}H_{28}F_5N_4O_6U$ $[M+H]^+$ requires 837.24314, found 837.25460 (mass error = 11.46 ppm), $C_{27}H_{27}F_5N_4O_6UNa$ $[M+Na]^+$ requires 859.22508, found 859.22830 (mass error = 3.22 ppm), $C_{27}H_{24}F_5N_4O_4U$ $[M-OAc]^+$ requires 777.22201, found 777.22640 (mass error = 5.64 ppm). EA for $C_{27}H_{27}F_5N_4O_6U$ (MW = 836.24 gmol^{-1}) requires C,38.77 %; H,3.25 %; N,6.70 %. Found C,38.83 %; H,3.35 %; N,6.51 %. FTIR (film) ν cm^{-1} 2962 (w), 2925 (w), 1590 (s), 1575 (s), 1520 (s), 1501 (s), 1495 (m), 1370 (m), 1352 (m), 1332 (w), 1292 (m), 1247 (s), 1199 (s), 1072 (m), 1005 (s), 979 (s), 951 (m), 905 (s), 837 (s), 805 (m), 758 (m), 743 (m), 725 (m), 713 (m), 645 (m). UV-vis (THF): λ 512 nm, ε = 20 812 M^{-1} cm^{-1}; λ_{max} 546.5 nm, ε = 82 316 M^{-1} cm^{-1}.

UO_2Cl(**L**) **Method A**: A solution of H**L** (131 mg, 0.257 mmol, 1 eq.; in MeOH:$CHCl_3$, 1:3, 150 mL) was added to a solution of $UO_2Cl_2THF_2$ (137 mg, 0.283 mmol, 1.1 eq.; in MeOH:$CHCl_3$, 1:3, 20 mL) after which NEt_3 was added (47 µL, 0.334 mmol, 1.3 eq.), causing an immediate colour change from orange to red. The reaction mixture was heated to 65 °C and stirred for 18 h, after which solvent was removed under reduced pressure. The majority of the red solid was redissolved in CH_2Cl_2 (400 mL) and filtered. The filtrate was washed with H_2O (3 x 50 mL) and dried with $MgSO_4$ and concentrated so obtain a red solid. The red solid and residue were combined yielding a red solid. Yield = 109 mg (91 %). ^{1}H NMR (400 MHz, Acetonitrile-d_3): δ_H 8.22 (2H, s), 7.46 (2H, d, J = 4.4 Hz), 7.19 (2H, d, J = 4.4 Hz), 1.76 (18H, s). ^{13}C{^{1}H} NMR (126 MHz, Acetonitrile-d_3): δ_C 169.78, 159.02, 144.81, 143.17, 142.42, 138.05, 137.56, 134.23, 132.34, 119.57, 55.02, 27.84. ^{19}F{^{1}H} NMR (376 MHz, Acetonitrile-d_3): δ_F –140.88 - –143.36, –154.28 - –155.13, –162.18 - –163.97. HRMS (ESI$^+$, MeOH): m/z $C_{25}H_{25}F_5N_4O_4ClU$ $[M+H]^+$ requires 813.19869, found 813.19580 (mass error = -2.89 ppm). FTIR (film) ν cm^{-1} 3300 (w), 3270 (w), 2972 (w), 1592 (s), 1570 (s), 1521 (s), 1489 (s), 1460 (m), 1374 (m), 1370 (m), 1348 (m), 1291(m), 1264 (s), 1200 (s), 1164 (m), 1075 (s), 1053 (w), 1007 (s), 974 (s), 978 (s), 950 (m), 912 (s), 839 (s), 804 (m), 771 (m), 743 (s), 726 (m), 714 (m), 647 (m). UV-vis (THF): λ 514 nm, ε = 18 582 M^{-1} cm^{-1}; λ_{max} 546 nm, ε = 84 301 M^{-1} cm^{-1}.

Method B: A solution of H**L** (35 mg, 0.068 mmol, 1.0 eq.) in dry THF (3 mL) was dropwise added to a slurry of KH (3 mg, 0.0746, 1.1 eq.) in dry THF (2 mL). The solution slowly turned pinkish red and was left stirred overnight after which it was dropwise added to a yellow slurry of $UO_2Cl_2THF_2$ (32 mg, 0.068 mmol, 1.0 eq.) in dry THF (2 mL), causing an immediate colour change from red to pink. The reaction mixture was stirred at room temperature for 18 hours, after which the reaction mixture was transferred to the bench and solved was removed under reduced pressure. The solid partially dissolved in CH_2Cl_2 (30 mL). The filtrate was washed with H_2O (3 x 3 mL), dried over $MgSO_4$ and concentrated. Both residue and washed filtrate were combined, obtaining a red solid.

$[Cp_2Co][UO_2(OAc)(\mathbf{L}^{\bullet})]$: A pink solution of $UO_2(OAc)$(**L**) (50 mg, 0.06 mmol, 1.0 eq.) in dry THF (5 mL) was added to a solution of $CoCp_2$ (11.3 mg, 0.06 mmol, 1.0 eq) in dry THF (1 mL). The solution turned dark greenish red instantaneously and a green precipitate started forming. The reaction was left stirring for 1 hr before centrifuging. Solis were obtained as a greenish brown solid. Yield = 46 mg (75 %). NMR silence. EPR S = ½, and g_{iso} of 1.997. EA for $C_{37}H_{37}CoF_5N_4O_6U$ (MW = 1025.25 gmol^{-1}) requires C,43.33 %; H,3.63 %; N,5.46 %. Found C,43.44 %; H,3.50 %; N,5.44 %. UV-vis (pyridine): λ 551 nm, ε = 10 500 M^{-1} cm^{-1}; λ_{max} 500 nm, ε = 45 700 M^{-1} cm^{-1}.

$[Cp_2Co][UO_2Cl(\mathbf{L}^{\bullet})]$: A pink solution of $UO_2(Cl)$(**L**) (49 mg, 0.06 mmol, 1.0 eq.) in dry THF (5 mL) was added to a solution of $CoCp_2$ (11.3 mg, 0.06 mmol, 1.0 eq) in dry THF (1 mL). The solution turned dark greenish red instantaneously and a green precipitate started forming. The reaction was left stirring for 1 hr before centrifuging. Solids were obtained as greenish brown solid. Yield = 55 mg (91 %). NMR silence. EPR S = ½, and g_{iso} of 1.997. EA for $C_{35}H_{34}ClCoF_5N_4O_4U$ (MW = 1002.09 gmol^{-1}) requires C,41.95 %; H,3.42 %; N,5.59 %. Found C,41.34 %; H,3.31 %; N,5.30 %. UV-vis (pyridine): λ 551 nm, ε = 10 500 M^{-1} cm^{-1}; λ_{max} 500 nm, ε = 45 700 M^{-1} cm^{-1}.

ASSOCIATED CONTENT

Supporting Information. Full synthetic procedures, X-ray crystallography, Density Functional calculations, EPR spectroscopy, and electrochemical methods. This material is available free of charge via the Internet at http://pubs.acs.org.

AUTHOR INFORMATION

Corresponding Author

*Jason.Love@ed.ac.uk

Author Contributions

The manuscript was written through contributions of all authors. / All authors have given approval to the final version of the manuscript.

Funding Sources

EPSRC (UK) Grant EP/L016419/1

Notes

The authors declare no competing financial interest.

ACKNOWLEDGMENT

The authors thank the University of Edinburgh, the EPSRC (UK), and the EPSRC CRITICAT Centre for Doctoral Training (PhD studentship to K.v.R.; Grant EP/L016419/1) for financial support. LM is a senior member of the Institut Universtaire de France. CalMip is acknowledged for a generous grant of computing time.

REFERENCES

1. Broere, D. L. J.; Plessius, R.; van der Vlugt, J. I., New avenues for ligand-mediated processes – expanding metal reactivity by the use of redox-active catechol, o-aminophenol and o-phenylenediamine ligands. *Chemical Society Reviews* **2015,** *44* (19), 6886-6915.
2. Dutta, S. K.; Beckmann, U.; Bill, E.; Weyhermüller, T.; Wieghardt, K., 1,2-Bis(pyridine-2-carboxamido)benzenate(2−), $(bpb)^{2-}$. A Noninnocent Ligand. Syntheses, Structures, and Mechanisms of Formation of $[(n\text{-Bu})_4N][Fe^{IV}_2(\mu\text{-N})(bpb)_2(X)_2]$ (X = CN^-, N_3^-) and the Electronic Structures of $[M^{III}(bpbox)(CN)_2]$ (M = Co, Fe). *Inorganic Chemistry* **2000,** *39* (15), 3355-3364.
3. Kraft, S. J.; Fanwick, P. E.; Bart, S. C., Synthesis and Characterization of a Uranium(III) Complex Containing a Redox-Active 2,2′-Bipyridine Ligand. *Inorganic Chemistry* **2010,** *49* (3), 1103-1110.
4. Coughlin, E. J.; Qiao, Y.; Lapsheva, E.; Zeller, M.; Schelter, E. J.; Bart, S. C., Uranyl Functionalization Mediated by Redox-Active Ligands: Generation of O–C Bonds via Acylation. *Journal of the American Chemical Society* **2019,** *141* (2), 1016-1026.
5. Pattenaude, S. A.; Mullane, K. C.; Schelter, E. J.; Ferrier, M. G.; Stein, B. W.; Bone, S. E.; Lezama Pacheco, J. S.; Kozimor, S. A.; Fanwick, P. E.; Zeller, M.; Bart, S. C., Redox-Active vs Redox-Innocent: A Comparison of Uranium Complexes Containing Diamine Ligands. *Inorganic Chemistry* **2018,** *57* (11), 6530-6539.
6. Halter, D. P.; Heinemann, F. W.; Maron, L.; Meyer, K., The role of uranium–arene bonding in H_2O reduction catalysis. *Nature Chemistry* **2018,** *10* (3), 259-267.
7. Crandall, H. W., The Formula of Uranyl Ion. *The Journal of Chemical Physics* **1949,** *17* (7), 602-606.
8. Cowie, B. E.; Purkis, J. M.; Austin, J.; Love, J. B.; Arnold, P. L., Thermal and Photochemical Reduction and Functionalization Chemistry of the Uranyl Dication, $[U^{VI}O_2]^{2+}$. *Chemical Reviews* **2019,** *119* (18), 10595-10637.
9. Herasymchuk, K.; Chiang, L.; Hayes, C. E.; Brown, M. L.; Ovens, J. S.; Patrick, B. O.; Leznoff, D. B.; Storr, T., Synthesis and electronic structure determination of uranium(VI) ligand radical complexes. *Dalton Transactions* **2016,** *45* (31), 12576-12586.
10. Bejger, C.; Tian, Y.-H.; Barker, B. J.; Boland, K. S.; Scott, B. L.; Batista, E. R.; Kozimor, S. A.; Sessler, J. L., Synthesis and characterization of a tetrathiafulvalene-salphen actinide complex. *Dalton Transactions* **2013,** *42* (19), 6716-6719.
11. Assefa, M. K.; Pedrick, E. A.; Wakefield, M. E.; Wu, G.; Hayton, T. W., Oxidation of the 14-Membered Macrocycle Dibenzotetramethyltetraaza[14]annulene upon Ligation to the Uranyl Ion. *Inorganic Chemistry* **2018,** *57* (14), 8317-8324.
12. Kent, G. T.; Murillo, J.; Wu, G.; Fortier, S.; Hayton, T. W., Coordination of Uranyl to the Redox-Active Calix[4]pyrrole Ligand. *Inorganic Chemistry* **2020,** *59* (12), 8629-8634.
13. Bolotaulo, D.; Metta-Magaña, A.; Fortier, S., F-element metalated dipyrrins: synthesis and characterization of a family of uranyl bis(dipyrrinate) complexes. *Dalton Transactions* **2017,** *46* (10), 3284-3294.
14. Pankhurst, J. R.; Bell, N. L.; Zegke, M.; Platts, L. N.; Lamfsus, C. A.; Maron, L.; Natrajan, L. S.; Sproules, S.; Arnold, P. L.; Love, J. B., Inner-sphere vs. outer-sphere reduction of uranyl supported by a redox-active, donor-expanded dipyrrin. *Chemical Science* **2017,** *8* (1), 108-116.
15. Bell, N. L.; Shaw, B.; Arnold, P. L.; Love, J. B., Uranyl to Uranium(IV) Conversion through Manipulation of Axial and Equatorial Ligands. *Journal of the American Chemical Society* **2018,** *140* (9), 3378-3384.
16. Takeyama, T.; Tsushima, S.; Takao, K., Effects of Substituents on the Molecular Structure and Redox Behavior of Uranyl(V/VI) Complexes with N_3O_2-Donating Schiff Base Ligands. *Inorganic Chemistry* **2021**.
17. Takao, K.; Tsushima, S.; Ogura, T.; Tsubomura, T.; Ikeda, Y., Experimental and Theoretical Approaches to Redox Innocence of Ligands in Uranyl Complexes: What Is Formal Oxidation State of Uranium in Reductant of Uranyl(VI)? *Inorganic Chemistry* **2014,** *53* (11), 5772-5780.
18. Shikha Singh, R.; Prasad Paitandi, R.; Kumar Gupta, R.; Shankar Pandey, D., Recent developments in metal dipyrrin complexes: Design, synthesis, and applications. *Coordination Chemistry Reviews* **2020,** *414*, 213269.
19. Baudron, S. A., Dipyrrin based metal complexes: reactivity and catalysis. *Dalton Transactions* **2020,** *49* (19), 6161-6175.
20. Thoi, V. S.; Stork, J. R.; Niles, E. T.; Depperman, E. C.; Tierney, D. L.; Cohen, S. M., Diamidodipyrrins: Versatile Bipyrrolic Ligands with Multiple Metal Binding Modes. *Inorganic Chemistry* **2008,** *47* (22), 10533-10541.
21. Jacobsen, J. A.; Stork, J. R.; Magde, D.; Cohen, S. M., Hydrogen-bond rigidified BODIPY dyes. *Dalton Transactions* **2010,** *39* (3), 957-962.
22. Saund, S. S.; Goldschmid, S. L.; Ng, K.; Stewart, V.; Siegler, M. A.; Thoi, V. S., Exploring ligand non-innocence of coordinatively-versatile diamidodipyrrinato cobalt complexes. *Chemical Communications* **2019,** *55* (12), 1825-1828.
23. Pankhurst, J. R.; Cadenbach, T.; Betz, D.; Finn, C.; Love, J. B., Towards dipyrrins: oxidation and metalation of acyclic and macrocyclic Schiff-base dipyrromethanes. *Dalton Transactions* **2015,** *44* (5), 2066-2070.
24. Brewster, J. T.; He, Q.; Anguera, G.; Moore, M. D.; Ke, X.-S.; Lynch, V. M.; Sessler, J. L., Synthesis and characterization of a dipyriamethyrin–uranyl complex. *Chemical Communications* **2017,** *53* (36), 4981-4984.
25. Clement, O.; Rapko, B. M.; Hay, B. P., Structural aspects of metal–amide complexes. *Coordination Chemistry Reviews* **1998,** *170* (1), 203-243.
26. Connelly, N. G.; Geiger, W. E., Chemical Redox Agents for Organometallic Chemistry. *Chemical Reviews* **1996,** *96* (2), 877-910.
27. Sheldrick, G. M., *Acta Crystallogr., Sect. A: Found. Adv.* **2015,** *71*, 3−8.
28. Sheldrick, G. M., *Acta Crystallogr., Sect. C: Chem.* **2015,** *71*, 3−8.
29. Sheldrick, G. M., *Acta Crystallogr., Sect. A: Found. Adv.* **2008,** (64), 122.
30. O. V. Dolomanov, L. J. B., R. J. Gildea, J. A. K. Howard, H. Puschmann, *J. Appl. Crystallogr.* **2009,** *42*, 339−341.

SYNOPSIS TOC